An infrared image dehazing method based on Modified Dark Channel Prior

Siyu Yan[a], Jingwen Zhu[b], Kai Yun[a], Yuexing Wang*[c], Chuangang Xu[c]
[a]College of Artificial Intelligence, No.38 Tongyan Road, Nankai University, Tianjin, CHN, 300350
[b]College of Software, No.38 Tongyan Road, Nankai University, Tianjin, CHN, 300350
[c]Tianjin Jinhang Institute of Technical Physics, No.58 Baoshui Road, Tianjin, CHN, 300192
* Corresponding author: 610064032@qq.com

ABSTRACT

To improve the effectiveness of the infrared image dehazing algorithm, we modify the DCP based on the observation of several outdoor haze-free images: in these images, pixels of most local patches no longer have low intensity but are close to high intensity. The transmission map is estimated through the MDCP, and the guided filter and CLAHE achieve enhancement. The haze infrared images can be recovered completely. Moreover, to thrive the infrared dehazing research, we introduce the IR Dense-haze dataset, which contains 13 pairs of synthetic haze infrared images and corresponding haze-free infrared images and six extra haze infrared images captured in natural scenes. Experiments on the IR Dense-haze dataset show that our method achieves dominant performance. The average PSNR of the infrared image is 39.02% higher than the original DCP method, and the average SSIM is 28.65% higher than the original DCP method.

Keywords: Dehazing; dark channel prior; pix2pix; guided filtering; dehazing dataset;

1. INTRODUCTION

Due to the solid anti-interference ability of radiation, infrared images offer a more remarkable ability to overcome visual obstacles than visible images, promoting their extensive utilization in the military field. However, the infrared images captured by the missile platform taken in adverse weather (e.g., hazy, foggy) commonly lose the contrast and details due to the effect of microparticles in the atmosphere. For these reasons, haze removal is highly desired in the academic field.

Most dehazing algorithms take the atmospheric scattering model[1] as the theoretical basis for dehazing. The DCP method[2] is based on the statistics of haze-free outdoor images, which show that some pixels have low intensity at least one channel. Many researchers have followed it and promoted its progress[3]. Liang et al. [4] utilized an adaptive double plateau histogram to achieve familiar results with DCP. Feng et al. [5] proposed a two-stage dehazing method based on DCP by exploiting the dissimilarity between the RGB and the IR image. Fang et al. [6] proposed a unified dehazing approach by analyzing the IR images captured under different weather conditions. However, these previous studies mainly focus on a small range of wavelengths of IR images. The lack of a general method for all IR images still exists. To date, most of the existing dehazing appraisal datasets [7,8] utilize known depth information and the simplified optical model to synthesize RGB hazy images. Luthen et al.[9] introduced a dataset containing only four pairs of indoor scenes and NIR images. Dense-Haze [10] contains 33 pairs of real hazy and corresponding haze-free images of various outdoor scenes. The focus in the dehazing dataset has been on RGB images which are potentially detrimental to IR image dehazing development.

In this paper, we propose an effective dehazing method for infrared image dehazing. (1) We modify the DCP to dehazing based on the observation of several outdoor haze-free images: in these images, pixels of most local patches are close to high intensity. (2) Unlike previous methods that only focus on a small range of wavelengths of infrared images, the proposed method has no limitation on the range of reprocessing images. (3) To thrive the infrared dehazing research, we introduce an IR Dense-Haze dataset containing 13 pairs of synthetic haze infrared images and corresponding haze-free infrared images and six extra haze infrared images captured in natural scenes.

The remainder of the paper is organized as follows. In Section 2, we review the atmospheric scattering model and DCP algorithm, which provides the basis of our method. In Section 3, we present details of the proposed method. In

Section 4, the IR Dense-Haze dataset is introduced. In Section 5, experimental results and a comparison with the existing methods are provided. Finally, conclusions are drawn in Section 6.

2. RELATED WORK

2.1 Atmospheric scattering model

To describe the formation of a haze image, an atmospheric scattering model[1] is developed as follows:

$$I(x) = J(x)t(x) + A(1 - t(x)) \tag{1}$$

where $I(x)$ is the captured image intensity, $J(x)$ represents the clear image with dehazing, and A and $t(x)$ denote the global atmospheric light and the medium transmission, respectively. x is the index of pixels. $t(x)$ represents the portion of the light that is not scattered into the acquisition device.

The former term of Eq.1, $J(x)t(x)$, is called direct attenuation. After the incident light reaches the target object, the light reflected scatters through the suspended microparticles in the atmosphere before reaching the acquisition device, deviating from the original reflection path and causing direct attenuation. The latter term, $A(1 - t(x))$ is called airlight. Target objects transmit reflected light to acquisition devices, scattering by particles and interference by sunlight-based ambient light. Obtaining an accurate estimation of medium transmission and global atmospheric light is essential for achieving haze removal.

2.2 dark channel prior

He et al.[2] proposed the dark channel prior method based on the observation of haze-free outdoor images that in most patches without a large area of sky, there exist pixels that have very low intensity even close to zero in at least one color channel, and these pixels are called dark channel pixels. It is mathematically denoted as follows:

$$J_{dark}(x) = min_{c\in(r,g,b)}(min_{y\in\Omega(x)}J_c(y) = 0 \tag{2}$$

where $J_c(y)$ represents a color channel of J and $\Omega(x)$ is a local godet centered on x with a specific size.

On the premise that assuming atmospheric light A is known, the formula for calculating t can be deduced from Eq.1 and Eq.2. Moreover, He et al. induced guided filtering[11] to optimize t. In addition, the pixels with the highest intensity in the dark channel are selected as the atmospheric light.

3. METHODOLOGY

3.1 Modified Dark Channel Prior

Because the imaging principle of infrared images is different from that of visible images, DCP cannot be directly utilized for infrared image dehazing. We modify the Dark Channel Prior for infrared image dehazing based on the observation on haze-free outdoor images: in most non-sky, non-meadow, and non-soil patches, pixels no longer have low intensity but close to high intensity (after extensive analysis, set the value as 180). The formula is redefined as follows:

$$J_{M-dark}(x) = min_{x\in\Omega(x)}J(x) = 180 \tag{3}$$

where $\Omega(x)$ is a local godet centered on x with a specific size, and x indexes pixels in the image J.

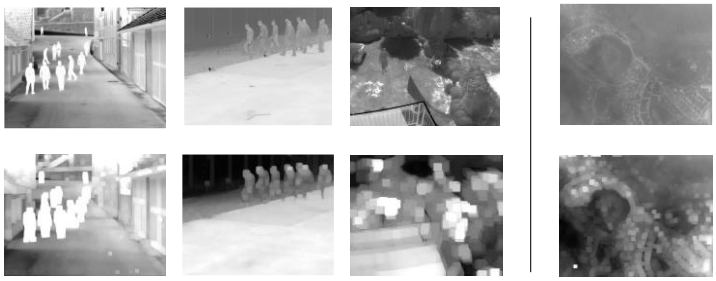

Figure 2. Left top: haze-free example images. Left Bottom: the corresponding M-dark channel. Right top: a haze image Right bottom: the corresponding M-dark channel.

We induce the LTRI dataset[12] to affirm our theory, which contains 20 thermal infrared sequences with 10068 infrared images. Under the condition that hazy always occurs outside, we pick out 6,927 IR images that nearly do not contain sky, meadow, or soil regions. The M-dark channel images are computed with a patch size of 15×15. Several infrared images and the corresponding M-dark channel images are shown in Fig. 2. Owing to the transmission of infrared radiation to light-haze, light-haze is difficult to reflect on infrared images. In other words, haze on infrared images is almost dense, leading to the haze image being darker than its haze-free version.

As shown in Fig. 3, we know that approximately 68% of the pixels in the M-dark channel image have values of approximately 180. The intensities of 80% are concentrated between 150 and 200. Therefore, we select 180.

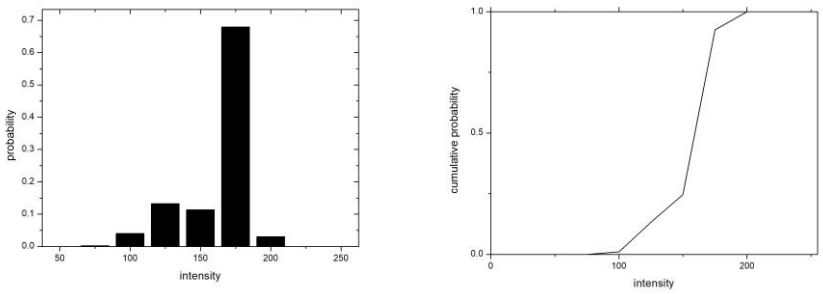

Figure 3. Statistics of the M-dark channel images. (a) Histogram of the intensity of the pixels in all 6,927 M-dark channel images (b) Corresponding cumulative distribution

3.2 Haze Removal Using the M-Dark Channel Prior

We adopt a rough calculation of the atmospheric light of a given hazy image proposed by He et al.[2]. Generally, the average of the highest 0.1% intensity was selected from the dark channel as the atmospheric light.

Estimating the transmission map from a single image is one of the significant tasks in the dehazing method. According to He et al.[2], first set the local patch $\Omega(x)$ as constant. Then taking the min operation on Eq.1, we have:

$$min_{y\in\Omega(x)}\left(\frac{I(y)}{A_c}\right) = t(x)min_{y\in\Omega(x)}(\frac{J(y)}{A_c})) + 1 - t(x) \tag{4}$$

As the M-dark channel prior we proposed, the M-dark channel image J_{M-dark} tends to be the value 180. Substituting Eq.3 into Eq.4, we can estimate the transmission map:

$$t(x) = \frac{A_c\left(1-min_{y\in\Omega(x)}I_c(y)\right)}{C-A_c} \tag{5}$$

To further optimize the transmission map, we induce the guided filter[11] and CLAHE[13]. This method dramatically reduces the processing time, solves the block effect, and makes the edge details of the image clearer. The guided filter is based on the assumption of a local linear model between the guidance I and the filtering output q. He et al.[11] assume that q is a linear transform of I in a window ω_x centered at pixel x:

$$q_i = \frac{1}{|\omega|}\sum_{x,i\in\omega_x} a_x I_i + b_x \tag{6}$$

where $|\omega|$ is the number of pixels in ω_x, and a_x and b_x are linear coefficients assumed to be constant in ω_x.

From $\nabla q = a\nabla I$, the local linear model guarantees that q produces the corresponding edges when window I have edges. The linear coefficients(a_x, b_x)are as follows :

$$a_x = \frac{\frac{1}{|\omega|}\sum_{i\in\omega_x} I_i p_i - \mu_x \bar{p}_x}{\sigma_x^2+\varepsilon} \tag{7}$$

$$b_x = \bar{p}_x - a_x\mu_x \tag{8}$$

where, μ_x and σ_x^2 are the mean and variance of I in ω_x while $\bar{p}_k$ is the mean of p_i in window ω_x. ε denotes the regularization parameter penalizing large a_x.

Then, we enhance the optimized transmission image utilizing CLAHE[13]. It is a method that enhances the contrast to preserve more details. CLAHE basically operates by limiting the contrast enhancement, which divides the images into several regions and applies HE[5] to each area. Put the optimized transmission map and *A* into Eq.1 and obtain the dehazed image. The diagram of the proposed method is shown in Fig.4.

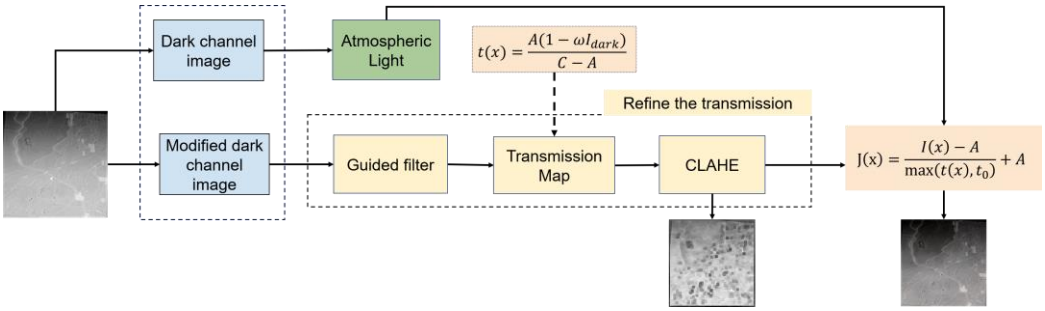

Figure 4. A representation of the proposed method.

4. IR DENSE-HAZE DATASET

We utilize pix2pix[14] to generate the haze images. Pix2pix is an advanced version of CGAN[15], which comprises a generator and a discriminator. It trains the transformation from the input image to the output image, and we utilize it to transform the color image to the infrared image in this paper. The discriminator calculates the similarity of the input image to the ground truth(or image synthesized by the generator) and classifies it as fake(synthesized by the generator) or true(the target image). The generator is updated to minimize the loss predicted by the discriminator and further generate pictures. The generator utilizes a U-Net architecture, while the PachGAN architecture is used as the discriminator. The structure of pix2pix is shown in Fig. 5.

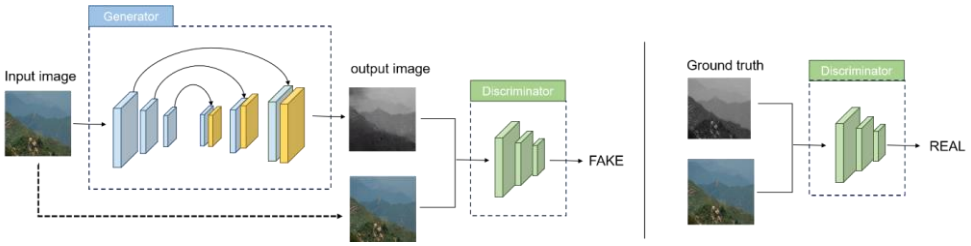

Figure 5. The structure of pix2pix.

Regarding the training data, we select the KAIST pedestrian dataset[16]. It consists of 95328 images, containing two versions of RGB color images and infrared images. The dataset captured various conventional traffic scenes, including campus, streets, and rural areas during the daytime and night. The image size is 640 × 480. Since this dataset is taken from the continuous frame image of the video, the adjacent images have nearly no difference, so we take one of every 30 pictures as the training set. After this operation, 3177 training set pictures can be obtained. Pix2pix is trained (1,200,000 iterations with a batch size of 32) on a PC with RTX 2060s. For the test dataset, we select the RESIDE-beta dataset [17], which contains 2061 outdoor haze images captured in Beijing. We select 300 pictures with more details and uniform haze concentration. Finally, images with better visual effects are selected into the dataset.

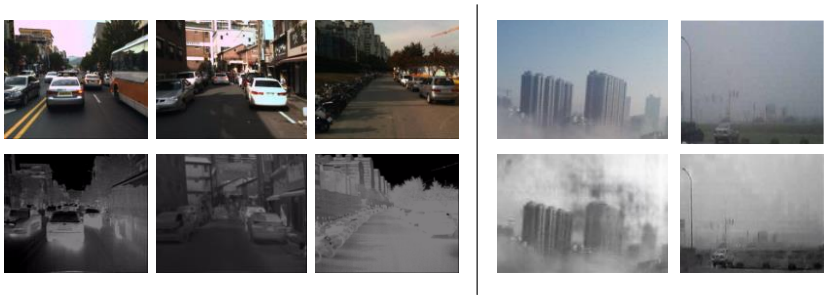

Figure. 6 Left: training data. Right: test results.

5. EXPERIMENTAL RESULTS

To verify the method, we select three classical traditional methods DCP[2], CAP[18], and CE[19] compared with our methods. In addition, GACNet[20] and Light-DehazeNet[21], which are based on deep learning methods are also compared with us. We selected hazy images with different concentrations as the test data, including two light-haze infrared images, one mid-haze infrared image, and one dense-haze infrared image. The last two are from the dataset we introduced. The results are explained both subjectively and objectively.

5.1 Subjective evaluation

We first analyze the results subjectively. The subjective feeling is directly using the human eye to observe the image, and it is convenient and intuitive.

Regarding the light-haze, as shown in Fig. 7 CAP[18], DCP[2] and Light-DehazeNet[21] exhibit brightness darkening and loss of detail information results. In the first scene, all is invisible except the object of the tree. The second is identical; the distant mountains are not visible after dehazing. GACNet[20] achieves an excellent dehazing effect but also loses some details. The river bank and car in the first image and the distant mountains in the second image are blurred. In addition to that, the haze-free region will exhibit brightness saturation and image quality decline. Compared to CE[19], our method achieves better detail enhancement and brightness recovery results. CAP[18] and DCP[2] are not dehazed completely for mid-haze. The result of Light-DehazeNet[21] has low brightness, which is not in line with human visual characteristics. GACNet[20], CE [19], and our method achieve good dehazing results. Thus, it is not easy to judge the overall quality of the visual effect. We will further evaluate the subsequent objective evaluation. For dense haze, as shown in Fig. 8, all algorithms are not ideal for removing dense haze.

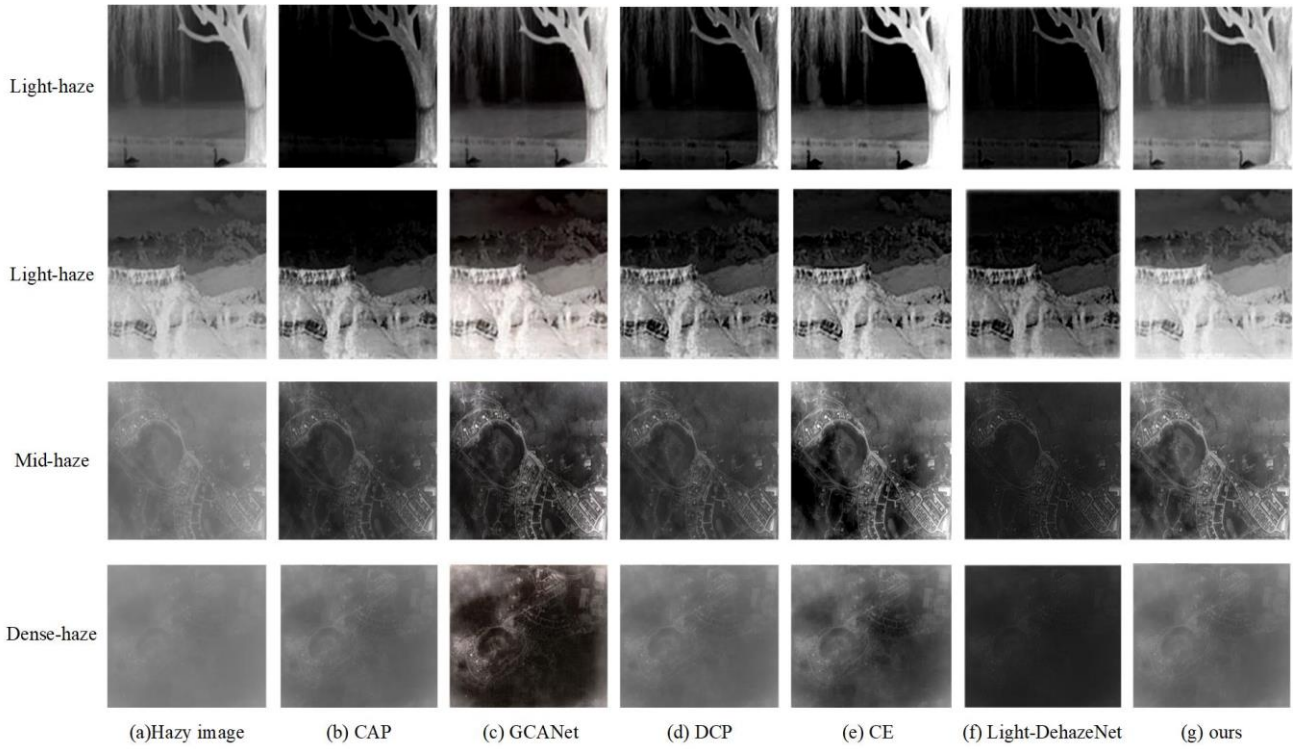

Figure. 7 Comparative results of selected single image dehazing methods

5.2 Objective Analysis

To objectively and fairly analyze the effectiveness of the algorithm, we adopt Absolute Mean Brightness, Peak Signal to Noise Ratio, and Structural Similarity as the Evaluation index. The parametric evaluation values calculated for selected images used in the previous section are displayed in Table 1.

For light-haze, our method achieves the highest SSIM value and PSNR value. In ABME, GACNet[20] and our method obtain the best results, respectively. For mid-haze, our method achieves all the best values, while DCP[2] arrives at the best results on dense-haze removal.

Table 1. Subjective evaluation.

Method	Haze	AMBE↓	PSNR↑	SSIM↑	Method	Haze	AMBE↓	PSNR↑	SSIM↑
CAP[18]	Light	73.7124	10.4268	0.1672	CE[19]	Light	3.9112	17.4172	0.6477
	Light	53.7077	13.0546	0.4839		Light	37.8703	15.8612	0.6800
	Mid	63.1048	12.0815	0.7429		Mid	43.1046	13.4075	0.6081
	Dense	19.6543	20.7438	0.9001		Dense	42.2576	14.7498	0.7868
	average	52.5449	14.0767	0.5735		average	31.7859	15.3589	0.6806
GACNet [20]	Light	14.9176	20.3886	0.7788	Light-DehazeNet [21]	Light	59.9233	11.8710	0.3108
	Light	**6.04914**	18.9523	0.8282		Light	63.3332	11.1879	0.4353
	Mid	62.8705	11.5842	0.5881		Mid	86.7133	9.2357	0.5014
	Dense	68.2047	10.6610	0.4825		Dense	87.9762	9.1256	0.5103
	average	38.0105	15.3965	0.6694		average	74.4865	10.3550	0.4394
DCP[2]	Light	59.7361	12.2583	0.4041	Proposed Algorithm	Light	**3.1868**	**35.6027**	**0.9927**
	Light	51.1339	13.5048	0.5869		Light	9.2661	**24.2554**	**0.9698**
	Mid	60.0319	12.4921	0.7466		Mid	**22.3709**	**19.4415**	**0.8682**
	Dense	**19.5695**	**21.9476**	**0.9511**		Dense	20.0809	21.4508	0.9373
	average	7.6178	15.0507	0.6721		average	13.7261	25.1876	0.9420

6. CONCLUSIONS

In this paper, we modify the DCP on the statistics of several outdoor haze-free infrared images and further provide a powerful image dehazing method, especially for infrared images. Experiments are partly conducted on IR Dense-haze dataset. Through the experimental results, we conclude that: (1) Our method achieves significant improvement over the original DCP method. (2) The current algorithms cannot process dense and inhomogeneous haze infrared images well. (3) The IR Dense-haze can afford the validation of the existing dehazing methods.

REFERENCES

[1] Narasimhan S G, Nayar S K. Vision and the atmosphere[J]. International journal of computer vision, 2002, 48(3): 233-254.

[2] He K, Sun J, Tang X. Single image haze removal using dark channel prior[J]. IEEE transactions on pattern analysis and machine intelligence, 2010, 33(12): 2341-2353.

[3] Liu S, Rahman M A, Wong C Y, et al. Dark channel prior based image de-hazing: A review[C]//2015 5th International Conference on Information Science and Technology (ICIST). IEEE, 2015: 345-350.

[4] Liang K, Ma Y, Xie Y, et al. A new adaptive contrast enhancement algorithm for infrared images based on double plateaus histogram equalization[J]. Infrared Physics & Technology, 2012, 55(4): 309-315.

[5] Feng C, Zhuo S, Zhang X, et al. Near-infrared guided color image dehazing[C]//2013 IEEE international conference on image processing. IEEE, 2013: 2363-2367.

[6] Fang T, Cao Z, Yan R. A unified dehazing approach for infrared images[C]//MIPPR 2013: Multispectral Image Acquisition, Processing, and Analysis. SPIE, 2013, 8917: 204-210.

[7] Ancuti C, Ancuti C O, De Vleeschouwer C. D-hazy: A dataset to evaluate quantitatively dehazing algorithms[C]//2016 IEEE international conference on image processing (ICIP). IEEE, 2016: 2226-2230.

[8] Zhang Y, Ding L, Sharma G. Hazerd: an outdoor scene dataset and benchmark for single image dehazing[C]//2017 IEEE international conference on image processing (ICIP). IEEE, 2017: 3205-3209.

[9] Lüthen J, Wörmann J, Kleinsteuber M, et al. A rgb/nir data set for evaluating dehazing algorithms[J]. Electronic Imaging, 2017, 2017(12): 79-87.

[10] Ancuti C O, Ancuti C, Sbert M, et al. Dense-haze: A benchmark for image dehazing with dense-haze and haze-free images[C]//2019 IEEE international conference on image processing (ICIP). IEEE, 2019: 1014-1018.

[11] He K, Sun J, Tang X. Guided image filtering[J]. IEEE transactions on pattern analysis and machine intelligence, 2012, 35(6): 1397-1409.
[12] Berg A, Ahlberg J, Felsberg M. A thermal object tracking benchmark[C]//2015 12th IEEE International Conference on Advanced Video and Signal Based Surveillance (AVSS). IEEE, 2015: 1-6.
[13] Khan S A, Hussain S, Yang S. Contrast enhancement of low-contrast medical images using modified contrast limited adaptive histogram equalization[J]. Journal of Medical Imaging and Health Informatics, 2020, 10(8): 1795-1803.
[14] Isola P, Zhu J Y, Zhou T, et al. Image-to-image translation with conditional adversarial networks[C]//Proceedings of the IEEE conference on computer vision and pattern recognition. 2017: 1125-1134.
[15] Mirza M, Osindero S. Conditional generative adversarial nets[J]. arXiv preprint arXiv:1411.1784, 2014.
[16] Hwang S, Park J, Kim N, et al. Multispectral pedestrian detection: Benchmark dataset and baseline[C]//Proceedings of the IEEE conference on computer vision and pattern recognition. 2015: 1037-1045.
[17] Li B, Ren W, Fu D, et al. Reside: A benchmark for single image dehazing[J]. arXiv preprint arXiv:1712.04143, 2017, 1.
[18] Zhu Q, Mai J, Shao L. A fast single image haze removal algorithm using color attenuation prior[J]. IEEE transactions on image processing, 2015, 24(11): 3522-3533.
[19] Kim J H, Jang W D, Sim J Y, et al. Optimized contrast enhancement for real-time image and video dehazing[J]. Journal of Visual Communication and Image Representation, 2013, 24(3): 410-425.
[20] Chen D, He M, Fan Q, et al. Gated context aggregation network for image dehazing and deraining[C]//2019 IEEE winter conference on applications of computer vision (WACV). IEEE, 2019: 1375-1383.
[21] Ullah H, Muhammad K, Irfan M, et al. Light-DehazeNet: A Novel Lightweight CNN Architecture for Single Image Dehazing[J]. IEEE Transactions on Image Processing, 2021, 30: 8968-8982.